

Wettability of Maleimide Copolymer Films: Effect of the Chain Length of *n*-Alkyl Side Groups on the Solid Surface Tension

K. Grundke,^{*,†} S. Zschoche,[†] K. Pöschel,[†] T. Gietzelt,[†] S. Michel,[†] P. Friedel,[†] D. Jehnichen,[†] and A. W. Neumann[‡]

Institute of Polymer Research, Hohe Strasse 6, D-01069 Dresden, Germany; and Department of Mechanical and Industrial Engineering, University of Toronto, 5 King's College Road, Toronto, Ontario, Canada M5S 3G8

Received December 20, 2000; Revised Manuscript Received June 18, 2001

ABSTRACT: We report bulk and surface properties of maleimide copolymers with two different backbones, poly(propene-*alt*-*N*-(*n*-alkyl)maleimides) (PAlkMI) and poly(styrene-*alt*-*N*-(*n*-alkyl) maleimides) (SAlkMI), with different lengths of *n*-alkyl side chains (methyl, ethyl, propyl, butyl, pentyl, hexyl, octyl, and dodecyl). The contact angle and solid surface tension results suggest that, for the longer side chains, the surface properties are dominated by the side chains. Indeed, the surface tension of the two types of copolymers with length of the side chain above $C = 6$ are essentially equal, indicating complete shielding of the polar backbone chain. For the two copolymers containing dodecyl side chains, the solid surface tension is similar to that of solid surfaces consisting exclusively of CH_3 groups. Apparently, these side groups are long enough to allow arrangement in the configuration of the lowest surface free energy possible for alkyl chains. For the short side chain copolymers the styrene compounds are more hydrophobic than the propene compounds. The bulkier phenyl rings shields the polar backbone chain more effectively than the small alkyl groups.

Introduction

Chemical modifications of polymer surfaces can be applied to control adhesion, wettability, and biocompatibility as important surface properties of polymers that are of interest for a variety of applications. The practical approaches to polymer surface modification include flame treatment, corona discharge treatment, plasma modification, and surface graft polymerization. Unfortunately, using these techniques, chemically well-defined surfaces cannot be designed and prepared.^{1,2}

Our approach is different in that surface functionalities are introduced by polymer analogous modification of alternating maleic anhydride copolymers with primary amines.^{3–5} In this way, maleimide copolymers can be obtained with the same degree of polymerization but different functionalities due to different side chains containing nonpolar or polar groups. An important property of these alternating copolymers is their thermal stability up to 300 °C.^{4,6} It should be mentioned that the synthesis of other stable polymeric systems, such as polyimides,^{7,8} polybenzimidazoles,⁹ or polybenzothiazoles,⁸ is demanding and often incompatible with functionalization. Moreover, these polymers are generally poorly soluble. The thermomechanical behavior of the alternating maleimide copolymers can be controlled by the substituent of the imide ring and by the type of comonomer.³ Maleimide copolymers with a very small substituent at the imide ring, such as methyl, give high glass transition temperatures (T_g). For maleimide copolymers with flexible alkyl side chains, lower T_g values are found due to the action of the latter as an intramolecular plasticizer.¹⁰

We report here bulk and surface properties of maleimide copolymers with two different backbones, poly-

(propene-*alt*-*N*-(*n*-alkyl)maleimides) (PAlkMI) and poly(styrene-*alt*-*N*-(*n*-alkyl) maleimides) (SAlkMI), and with different lengths of *n*-alkyl side chains (methyl, ethyl, propyl, butyl, pentyl, hexyl, octyl, and dodecyl). The abbreviations used for these copolymers are as follows: PMeMI, PEtMI, PPrMI, PBuMI, PPeMI, PHeMI, POcMI, and PDoMI and SMeMI, SEtMI, SPrMI, SBuMI, SPeMI, SHeMI, SOcMI, and SDOMI, respectively. Since the maleimide copolymers have good film forming properties, thin films were prepared on silicon wafers and their wettability was determined by contact angle measurements. It has been shown that under certain conditions, i.e., smoothness and homogeneity of the surfaces and constancy of the advancing contact angles, the contact angle is compatible with Young's equation and a unique expression of polymer properties.¹¹ Under these circumstances, the solid surface tension can be calculated from experimental (Young) contact angles and liquid surface tensions using the equation of state approach for interfacial tensions.^{11,12} The question arises how the solid surface tension of the maleimide copolymers reacts to the systematic change in the bulk structure. The bulk structure has been investigated by wide-angle X-ray scattering (WAXS), differential scanning calorimetry (DSC) and infrared spectroscopy (FTIR). In addition, molecular modeling was used to elucidate the molecular conformation of the macromolecules.

In the case of solid polymer surfaces, it is often assumed that a high-molecular-weight polymer creates a surface populated by the side chain groups attached to the polymer backbone.¹³ Many fluorinated side groups have been introduced to block copolymers to study their influence on the surface properties of these materials.^{14–19} Wang et al.¹⁸ studied systematically the influence of the chemical structure of poly(styrene-*b*-semifluorinated side chain) block copolymers on the critical surface tension of these polymers by varying the relative lengths of the fluorocarbon and hydrocarbon units in the side

* To whom correspondence should be sent. Telephone: ++49 351 4658 475. Fax: ++49 351 4658 284. E-mail: grundke@ipfdd.de.

[†] Institute of Polymer Research.

[‡] University of Toronto.

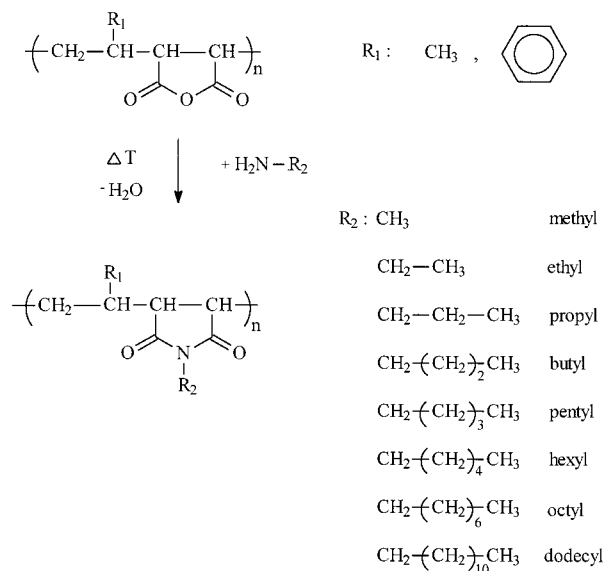
group. The block copolymers were synthesized by anionic polymerization of poly(styrene-*b*-1,2/3,4-isoprene) followed by the appropriate polymer analogous reactions. The only difference in the resulting polymers was the nature of the fluorinated side chain. This approach was used to judge the influence of the side group on the surface properties of the block copolymers. In comparison to liquid crystalline coil block copolymers with conventional side group mesogens, semifluorinated side chain block copolymers exhibit a more pronounced ability to organize in both organic solution and the solid state. For the same block copolymer, longer fluorocarbon side chains $-(CF_2)_{10}-$ produced a lower critical surface tension. The water contact angle was about 12° higher compared to a side chain containing only $-(CF_2)_6-$ ($\theta_a = 111^\circ$). The critical surface tension (8 mJ/m^2) obtained for the $-(CF_2)_{10}-$ side chain block copolymer was very close to that for a LB film surface of the corresponding perfluorocarbon acid. $-\text{CH}_2-$ spacer groups did not have a large effect on the surface tension, but longer $-\text{CH}_2-$ spacer groups rendered the semifluorinated side chain packing more stable and the block copolymer became more soluble.

Marra et al.^{20–22} synthesized copolymers of poly-(amide urethanes) and investigated the influence of fluorocarbon- and siloxane-containing side chains on the critical surface tension of thin films prepared by spin casting or dip coating. From X-ray photoelectron spectroscopy analysis, they concluded that the fluorocarbon side chains orient at the surface of the polymer films to create a low-energy surface.²³ From the study of water contact angles and critical surface tensions as a function of side chain siloxane length, they conclude that the PDMS-containing side chains phase segregate to expose the low-energy siloxanes at the surface.²²

In previous studies, we prepared thin films of poly-(4-*X*-styrenes) and polymethacrylates to investigate the influence of different substituents [$X = \text{H}, \text{CH}_3, \text{C}(\text{CH}_3)_3, \text{Cl}, \text{and OH}$]²⁴ and different alkyl side chains (methyl, ethyl, *n*-butyl, and *tert*-butyl)²⁵ on the solid surface tension of these materials. It was found that increasing length and size of the alkyl side chain decreases the solid surface tension, as expected. However, with increasing chain length of the alkyl side chain, the capability of reducing the solid surface tension was less pronounced. It appears that the polar polymethacrylate backbone was shielded by the alkyl side chain and its influence on the surface tension diminishes as the length and size of the alkyl chain increases. On the basis of this finding, it has to be expected that increasing the length of the side chains further should lead to a limiting value of the surface tension. The interesting question that arises is how many methylene groups are needed to reach that point.

It is the purpose of this study to explore further the relationship between the molecular structure of polymers, the exposure of molecular groups at the surface, and the effect on the solid surface tension. The present paper presents a detailed study of the effect of chain length of *n*-alkyl side groups in maleimide copolymers with different backbones on the wettability of thin films prepared from these copolymers. The wettability was determined by contact angle measurements using axisymmetric drop shape analysis—profile (ADSA—P). In previous contact angle studies^{5,26,27} using films of selected maleimide copolymers, it was shown that these surfaces were not inert with respect to certain liquids.

Scheme 1. Reaction Scheme of the Synthesis of Poly(propene-*alt*-*N*-(*n*-alkyl)maleimides) (PAlkMI) and Poly(styrene-*alt*-*N*-(*n*-alkyl)maleimides) (SAlkMI)



Therefore, caution has to be exercised when measuring and interpreting contact angles. It was also shown in previous articles that low-rate dynamic contact angle measurements from ADSA—P allow one to distinguish between thermodynamically relevant contact angles—i.e., contact angles which can be used in the Young equation—from very complex contact angle responses for some solid–liquid systems.¹¹ In the present study, we use water and glycerol for the contact angle measurements. Both liquids were found to give constant and hence meaningful advancing contact angles. These contact angles were used to calculate the solid surface tension by the equation of state approach for solid–liquid interfacial tensions.^{11,12}

Experimental Section

Synthesis of Maleimide Copolymers. Maleimide copolymers were synthesized by modification of alternating maleic anhydride copolymers, poly(propene-*alt*-maleic anhydride) and poly(styrene-*alt*-maleic anhydride), with primary amines (methyl-, ethyl-, propyl-, butyl-, pentyl-, hexyl-, octyl-, or dodecyl-amine).³ Due to this polymer analogous modification, maleimide copolymers with the same degree of polymerization but different side chains could be prepared. The molecular weights of the poly(propene-*alt*-maleic anhydride) determined by gel permeation chromatography are $M_w = 27\,300$ and $M_n = 9700$ and poly(styrene-*alt*-maleic anhydride) $M_w = 54\,000$ and $M_n = 19\,300$, respectively.³ The formation of the stable imide ring, accompanied by water production, proceeds almost quantitatively in a two-step reaction involving acid/amide as an intermediate product. Excess of primary amines was used in the modification of the copolymers. The maleimide copolymers were produced through a reaction of poly(propene-*alt*-maleic anhydride) and poly(styrene-*alt*-maleic anhydride), respectively, with the appropriate alkylamines in acetic acid at 118°C over 5–6 h. For purification, the copolymers were precipitated from a tetrahydrofuran (THF) solution in hexane and dried in a vacuum at 30°C . Subsequently, the copolymers were dissolved in THF and precipitated using *n*-hexane. This procedure was repeated several times. The reaction scheme is given in Scheme 1. As an illustration, Figure 1 shows ATR–FTIR spectra for POcMI and SOcMI. The carbonyl bands of the imide groups occur at 1692 and 1770 cm^{-1} indicating the essentially complete reaction to the imides.

Film Preparation. The copolymer films were prepared on oxide covered Si (100) wafers (Wacker Siltronic) by a solvent

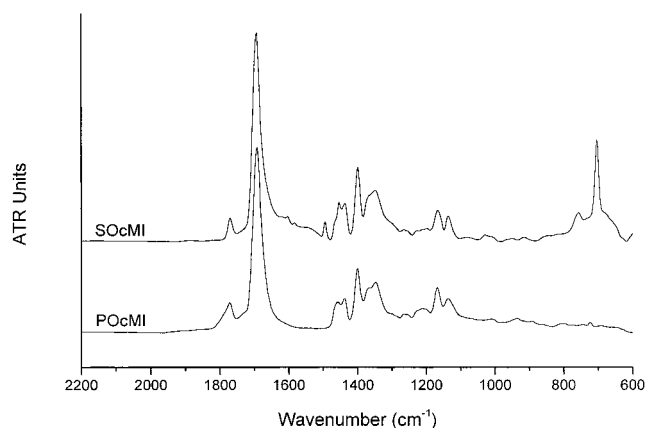


Figure 1. ATR-FTIR spectra of poly(styrene-*alt*-*N*-(*n*-octyl)-maleimide) (SOcMI) and poly(propene-*alt*-*N*-(*n*-octyl)-maleimide) (POcMI).

casting procedure in the case of PAlkMI and by spin coating in the case of SAlkMI (Headway Inc.; 2000 rpm for 30 s) using a 2% solution of the copolymer in tetrahydrofuran (Sigma-Aldrich, 99.9+% HPLC). In the case of solvent casting, a few drops of the 2% polymer/tetrahydrofuran solution were placed on silicon wafer substrates. The solution spread and the solvent was allowed to evaporate slowly inside Petri dishes for 48 h at room temperature. The films were then dried in a vacuum for 12 h at room temperature. Before coating, the silicon wafers were cleaned using a mixture of H₂SO₄ and H₂O₂ (3:1) at 80 °C for 1 h, rinsed with Millipore water for 30 min, and dried in a vacuum before polymer coating. After spin coating, the films were dried for 12 h at room temperature in a vacuum. Very smooth surfaces of the copolymers were obtained. The roughness was in the order of several nanometers on a micrometer length scale as determined by atomic force microscopy ($R_a = 0.4$ nm).

Contact Angle Method. Axisymmetric drop shape analysis—profile (ADSA-P) was used to determine the contact angles from the shape of axisymmetric sessile drops. The strategy employed is to fit the shape of an experimental drop to a theoretical drop profile according to the Laplace equation of capillarity, using the surface tension as an adjustable parameter.

With respect to the low-rate dynamic contact angle measurements by ADSA-P, liquid is supplied to the sessile drop from below the solid surface using a motorized syringe device. It is a good strategy^{11,26} first to deposit a very small drop of liquid over the small hole which is needed to supply liquid from below. This avoids hinging of the advancing drop on the lip of the hole. The experimental procedure of growing the drop from below is necessary since ADSA determines the contact angles based on a complete and undisturbed drop profile.

While the drop is growing at very slow motion of the three-phase contact line, a sequence of images is recorded by the computer (typically one image every 2–5 s). Since ADSA-P determines the contact angle and the three-phase contact radius simultaneously for each image, the advancing and receding dynamic contact angles as a function of the three-phase contact radius (i.e., location on the surface) can be obtained. Furthermore, the liquid surface tension is determined for each image, and can also be recorded. Details of the ADSA methodology, procedure, and experimental setup for low-rate dynamic contact angle measurements are given elsewhere.^{5,11,24–31} During the contact angle experiments the temperature and relative humidity were maintained, respectively, at 23 ± 0.5 °C and about 40%.

Results and Discussion

Bulk Properties. The glass transition temperatures of the copolymers were determined by DSC and are listed in Table 1. As expected, the T_g values for the styrene copolymers are significantly higher than those

Table 1. Glass Transition Temperatures of Poly(propene-*alt*-*N*-(*n*-alkyl)maleimides) and Poly(styrene-*alt*-*N*-(*n*-alkyl)maleimides)

<i>n</i> -alkyl side chain	T_g (°C)	
	poly(propene- <i>alt</i> -MI)	poly(styrene- <i>alt</i> -MI)
methyl	162	204
ethyl	151	195
propene	120	171
butyl	102	154
pentyl	82	141
hexyl	69	122
octyl	59	110
dodecyl	42	77

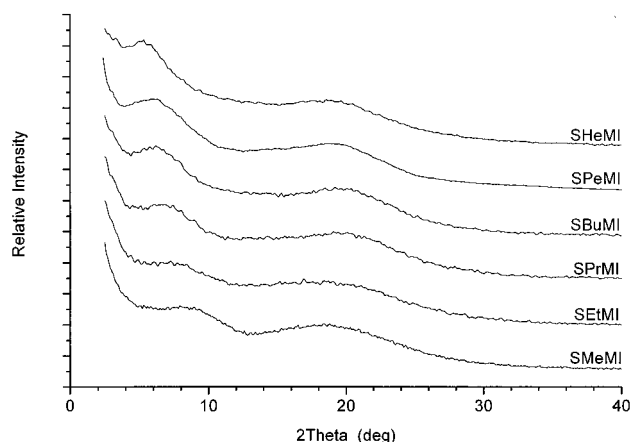


Figure 2. WAXS pattern of poly(styrene-*alt*-*N*-(*n*-alkyl)-maleimides) with different alkyl side chains (shifted scattering curves).

Table 2. d Value of Maximum Obtained by WAXS Experiments and Increase per CH₂ Unit for Poly(styrene-*alt*-*N*-(*n*-alkyl)maleimides)

poly(styrene- <i>alt</i> - <i>N</i> -(<i>n</i> -alkyl)maleimide)	d value of max (nm)	increase per CH ₂ unit (nm)
SMeMI	0.99	0.07
SEtMI	1.06	0.16
SPrMI	1.22	0.12
SBuMI	1.34	0.11
SPeMI	1.45	0.13
SHeMI	1.58	

of the corresponding propene copolymers. Also, as expected, the T_g decreases with increasing length of the side chains, since these chains act as a kind of internal plasticizer.

The results of wide-angle X-ray diffraction experiments (WAXS) on selected poly(styrene-*alt*-*N*-maleimides) are shown in Figure 2. The distance d between copolymer chains and the increase in diameter with increasing length of the side chains are given in Table 2. It can be seen that the increase in diameter of the structure from the methyl to the ethyl side group is 0.07 nm, and almost twice that for the subsequent steps, on average. This is plausible in the light of the molecular modeling results below, since the methyl and ethyl side chains do not protrude significantly from the space taken up by the phenyl ring of the comonomer styrene. For the longer side chains the increase in the d value with each additional CH₂ unit corresponds well with the increase of an alkyl chain in the zigzag confirmation, i.e., 0.125 nm. It is interesting to note that the much smaller increase in the d value when going from SMeMI to SEtMI is also reflected in the decrease of T_g values with increasing length of the side chains, cf. Table 1. From SMeMI to SEtMI the decrease in the T_g is 9 K,

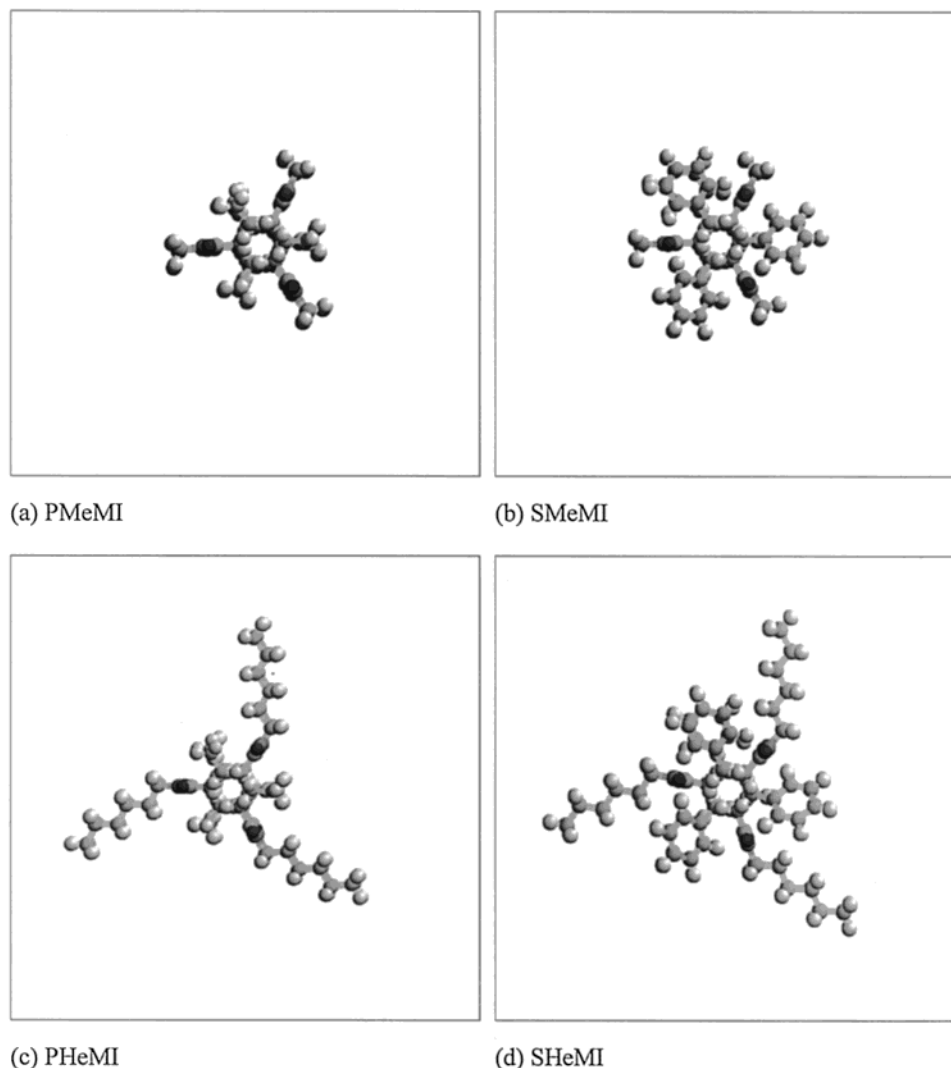


Figure 3. View onto the helical molecular polymer structure as obtained by molecular modeling for two methyl- (a and b) and two hexyl- (c and d) maleimide side chain copolymers.

whereas for the step from SEtMI to SPrMI is 24 K. This pattern is also observed for the PAlkMI copolymers.

To obtain a better comprehension of the steric arrangement of the copolymer chains, molecular models were constructed. The geometry and molecular conformation of the monomer units in the maleimide copolymers were optimized using a software package (GAMESS1)³² for quantum mechanical ab initio calculations. Single polymer chains were built using a software package called (BUILDER2),³³ an interpreter that connects atomic models of residues to build blocks and then to link blocks to a chosen degree of polymerization. Figure 3 shows views onto the helical molecular polymer structure of the two types of copolymers possessing a methyl or a *n*-hexyl side chain. The molecular conformation (calculated for vacuum conditions at 0 K) is built by phenyl rings at styrene units arranged in a comblike structure. Around one aromatic ring in the middle three phenyl rings are arranged with an angle of 120°. This structure is energetically favorable. The maleimide rings are tilted by 90° with respect to the phenyl rings. In this way, phenyl and maleimide rings do not hinder each other. This arrangement leads to a helixlike structure of the macromolecules. The second part of the structure is built by the side chains. In the middle of the comblike arranged phenyl rings or propene mono-

mers, the side chains grow starting at the maleimide rings. Longer side chains exceed the structure formed by the phenyl rings or propene units.

Surface Properties. Figures 4 and 5 represent typical contact angle results on films of POcMI for water and glycerol, respectively, obtained by ADSA-P. Because of the constant volume flow rate, the drop volume *V* as measured by ADSA increases linearly. As a consequence, the contact radius *R* of the sessile drop also increases monotonically and indeed roughly linearly, at a rate of approximately 0.2 mm/min.

During this process the contact angle θ remains essentially constant as the drop advances, at a value near 94° for water (Figure 4) and near 87° for glycerol (Figure 5). It is well-known that this contact angle is independent of the rate of advance on smooth surfaces, at least up to a rate of 1 mm/min.^{11,28} As the pump is reversed after approximately 500 s, the drop volume starts to decrease linearly. The contact angle decreases rapidly, at constant drop contact radius *R*; i.e., the drop hinges on the largest contact radius reached. At a certain point, at approximately 800 s, the three-phase line detaches and starts moving inward. Interestingly, the contact angle keeps decreasing; i.e., there is no constant, unique receding contact angle. The cause for this effect is believed to be liquid retention of the liquid

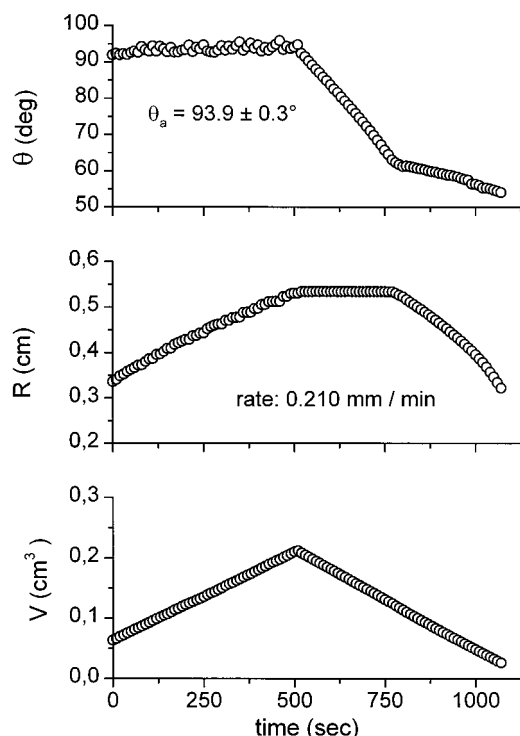


Figure 4. ADSA contact angle measurements of water on POCMI. θ is the contact angle, R is the contact radius of the sessile drop, the rate is the rate of motion of the three-phase line, and V is the drop volume.

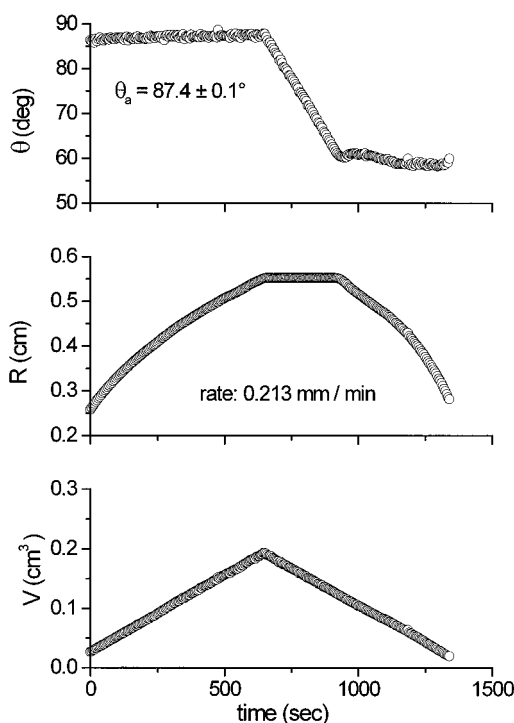


Figure 5. ADSA contact angle measurements of glycerol on POCMI. θ is the contact angle, R is the contact radius of the sessile drop, the rate is the rate of motion of the three-phase line, and V is the drop volume.

on the polymer surface, and possibly sorption and swelling processes of the polymer film.^{29,30} The decrease of the contact angle with the time of contact between liquid and polymer surface makes this type of mechanism plausible. It has been shown that the constancy of the advancing contact angles indicates compatibility with Young's equation. Thus, the advancing contact

Table 3. Summary of Low Rate Dynamic Advancing Contact Angles of Water and Glycerol on PAlkMI Copolymer Surfaces^c

copolymer <i>n</i> -alkyl side chain	water θ (deg)	glycerol θ (deg)
methyl	69.3	59.6
	70.4	59.4
	mean: 69.8 ± 0.8	59.5 ± 0.1
	69.8 ± 0.4^a	60.2 ± 0.4^a
ethyl	73.4	64.3
	73.9	65.4
	74.5	
	mean: 73.9 ± 0.6	64.8 ± 0.8
propyl	77.6	71.2
	78.9	70.8
	mean: 78.2 ± 0.9	71.0 ± 0.3
	77.5 ± 0.3^b	70.7 ± 0.2^b
butyl	(81.6)	75.1
		73.6
	mean:	74.3 ± 1.1
	88.0	
pentyl	91.7	
	88.2	
	86.1	
	87.5	
hexyl	86.4	
	mean: 88.0 ± 0.8	
	93.0	(81.4)
	92.5	
octyl	mean: 92.8 ± 0.4	
	92.3 ± 0.2^b	82.8 ± 0.3^b
	93.9	87.2
	97.0	87.4
dodecyl	98.0	
	94.4	
	mean: 95.8 ± 2.0	87.3 ± 0.1
	98.6	94.2
	98.3	91.6
	98.9	91.6
	99.2	92.0
	100.6	93.5
	99.4	96.2
	99.2	95.1
	100.1	96.5
	100.3	92.7
	99.7	
	mean: 99.4 ± 0.7	93.7 ± 1.9

^a Reference 27. ^b Reference 26. ^c The error limits are standard deviations. Copolymer films were produced by solvent casting.

angle is a unique expression of polymer surface properties.^{11,26,28} Since we are interested here in the surface energetic characterization of polymers and not in study of liquid penetration into the polymer films, only advancing contact angles will be considered and interpreted in terms of the solid surface tension. Figure 5 shows that very similar contact angle patterns are observed using glycerol as the sessile liquid drop.

Table 3 contains the contact angle results obtained on PAlkMIs surfaces for water and glycerol. Up to 10 runs of the type shown in Figures 4 and 5, on a new surface each time, were performed. The average advancing contact angles, as illustrated for one run in Figures 4 and 5, are given, together with the mean value for each copolymer. The error limits are standard deviations throughout. The standard deviations for the contact angles for each individual run are very small, typically in the range 0.1–0.3°. This is in part due to the fact that very large numbers of individual contact angles, each for a new drop, can be acquired in a run. However, the small values of the standard deviation for each run also attest to the uniformity of the polymer films. Interestingly, the errors from averaging over all runs are somewhat larger. Presumably this is due to

the fact that, despite all the care taken with the preparation of the films, there is a somewhat larger variability from film to film than on an individual film. For three of these copolymers, i.e., PMeMI, PPrMI, and PHeMI, literature values for the contact angles exist^{26,27} and are also given in Table 3. These measurements were performed using the same polymer materials (same charges). The polymer surfaces had been prepared by solvent casting of a 2% copolymer/tetrahydrofuran solution. The agreement between the two sets of data from two different laboratories is excellent, seen on the background that standard literature still suggests that the reproducibility of contact angle measurements is $\pm 2^\circ$ at best. As a very minor point, we note that the error limits in refs 26 and 27 are the 95% confidence limits. The main result of the summary of the contact angles for the poly(propene-*alt*-*N*-(*n*-alkyl)maleimides) shown in Table 3 is the monotonic increase of the contact angle with increasing length of the *n*-alkyl side chain.

The contact angle results for the SAlkMIs are given in Table 4. It should be noted that the polymer films for this family of copolymers were prepared by spin coating and not by solvent casting, as in the case of the PAlkMI copolymers. Preliminary experiments had shown that the SAlkMI copolymers yielded relatively poor quality solvent cast films with concomitant difficulties with reproducibility of the contact angles, particularly for the longer side chains. To illustrate that the two different procedures do not yield energetically different surfaces, the results of measurements with films of SMeMI obtained by film casting, which proved to be marginally satisfactory, are given in Table 5. It is apparent that, statistically speaking, the same average contact angles is obtained as in Table 4, albeit with a much larger error limit, illustrating the lower quality of films obtained by film casting. It can be seen for this type of copolymers too that the hydrophobicity increases with increasing length of the *n*-alkyl side chain.

The tendencies mentioned above are better appreciated in the plots of the contact angle data over the length of the *n*-alkyl side chains for both types of polymers in Figures 6 and 7, respectively. It is apparent in Figure 6 that the hydrophobicity of the PAlkMI copolymers increases more or less linearly up to a length of the alkyl side chain of $C = 6$ and then flattens out rapidly, suggesting that a limiting value of the contact angle would be reached for very long side chains. Contrary to the pattern for the bulk properties, cf. Tables 1 and 2, the contact angles in Figure 6 change smoothly from PMeMI to PHeMI, i.e., there is no difference between the contact angle change from PMeMI to PEtMI and the subsequent steps. This is quite plausible since, at the surface, the methyl groups are just as accessible for interaction with liquid molecules as the longer side chains. The SAlkMI copolymers are more hydrophobic already at short *n*-alkyl side chain length and approach a limiting value of the contact angle more gradually as the length of the side chain increases (see Figure 7). It is interesting to note in Figure 7 that there is some indication of an odd/even effect at short chain length: The contact angles for $C = 2$ and $C = 3$ as well as the angles for $C = 4$ and $C = 5$ are very similar. Effects of this type are well-known for other physical properties as well.

The advancing contact angles were used to calculate the solid surface tensions γ_{sv} for all maleimide copoly-

Table 4. Summary of Low Rate Dynamic Advancing Contact Angles of Water on SAlkMI Copolymer Surfaces^a

copolymer <i>n</i> -alkyl side chain	water θ (deg)
methyl	80.2
	80.5
	80.3
	79.7
	79.9
	79.9
	mean: 80.1 ± 0.3
	85.2
	84.9
	85.7
ethyl	82.7
	84.1
	83.8
	84.9
	mean: 84.5 ± 1.0
	85.7
	86.2
	86.5
	86.6
	85.2
propyl	85.0
	83.7
	mean: 85.6 ± 1.0
	90.4
	89.6
	91.2
	90.8
	90.0
	mean: 90.4 ± 0.6
	89.0
pentyl	90.4
	90.8
	91.5
	91.8
	90.8
	90.1
	91.0
	mean: 90.7 ± 0.7
	94.0
	93.7
hexyl	93.5
	95.0
	91.0
	93.0
	mean: 93.4 ± 1.3
	97.7
	97.3
	97.2
	94.8
	mean: 96.8 ± 1.3
dodecyl	101.0
	101.0
	101.5
	100.6
	99.9
	100.8
	mean: 100.8 ± 0.5

^a The error limits are standard deviations. Copolymer films were produced by spin casting

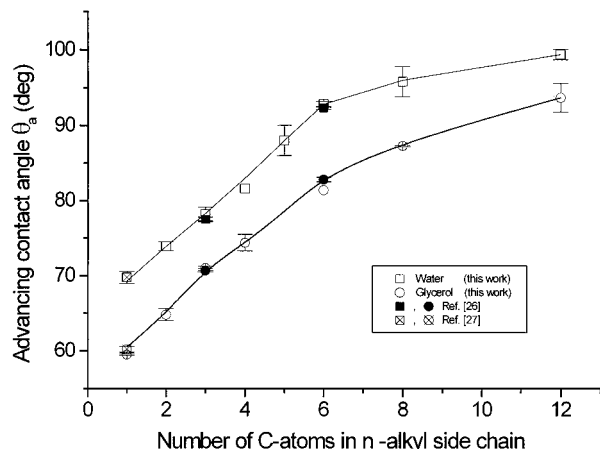
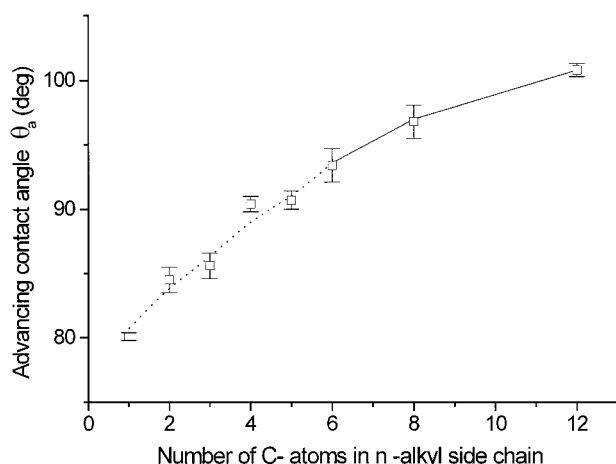
mer surfaces studied in the usual way from the equation of state for interfacial tensions.^{11,28} The results for PAlkMIs are given in Table 6 and those for the SAlkMIs in Table 7. The differences between the γ_{sv} values calculated with water and glycerol (Table 6) are within the range of scatter normally observed in such contact angle studies.¹¹

The average values of solid surface tensions for the PAlkMI copolymers and the values for the SAlkMI copolymers obtained from the contact angle measurements with water are plotted over the chain length of the *n*-alkyl side chains in Figure 8. These results

Table 5. Low Rate Dynamic Advancing Contact Angles of Water on SMeMI Copolymer Surfaces^a

copolymer <i>n</i> -alkyl side chain	water θ (deg)
methyl	79.5
	76.6
	83.3
	80.2
	79.6
	mean: 79.8 ± 2.4

^a The error limit is the standard deviation. Copolymer films were produced by solvent casting.

**Figure 6.** Mean of the advancing contact angles of water and glycerol as a function of the alkyl side chains for the PAlkMI copolymers.**Figure 7.** Mean of the advancing contact angles of water as a function of the alkyl side chains for the SAlkMI copolymers.

suggest the following, in conjunction with Figure 3. For the very short side chains, the phenyl group of the SAlkMI copolymers partially shields the very polar maleimide group. The surface tension of the PMeMI and PEtMI copolymers is similar to that of some polyamides.³⁴ By comparison, the surface tension of polystyrenes is near 30 mJ/m².^{24,31} With increasing length of the side chain, the two types of copolymers become more similar in surface tension. This suggests that the side chains screen not only the very polar backbone chain but eventually the styrene group as well. At *C* = 6 the surface tension of the two types of polymers has become almost the same. With further increasing length of the side chains, the surface tension of the copolymers decreases only slowly and apparently tends toward some final value. Interestingly, the *T_g* values, see Table 1,

Table 6. Summary of Solid Surface Tension γ_{sv} of PAlkMI Calculated from Mean Advancing Contact Angles of Water ($\gamma_{lv} = 72.2$ mJ/m²) and Glycerol ($\gamma_{lv} = 63.1$ mJ/m²)^a

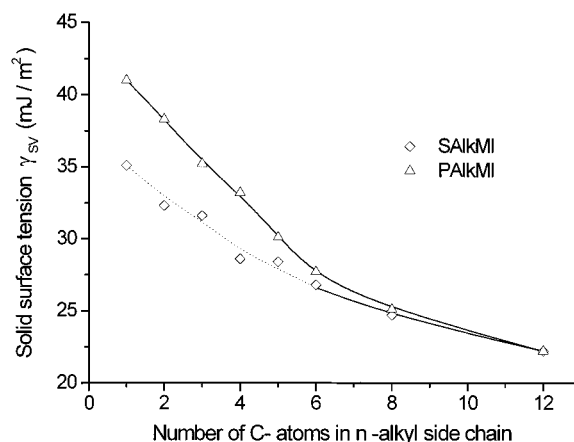
copolymer <i>n</i> -alkyl side chain	$\gamma_{sv}(\text{water})$ (mJ/m ²)	$\gamma_{sv}(\text{glycerol})$ (mJ/m ²)	$\gamma_{sv}(\text{mean})$ (mJ/m ²)
methyl	41.4 ± 0.5	40.7 ± 0.1	41.0
ethyl	38.9 ± 0.4	37.7 ± 0.5	38.3
propyl	36.2 ± 0.6	34.2 ± 0.2	35.2
butyl	34.1	32.3 ± 0.7	33.2
pentyl	30.1 ± 0.5		30.1
hexyl	27.1 ± 0.3	28.2	27.7
octyl	25.3 ± 0.7	24.9 ± 0.6	25.1
dodecyl	23.1 ± 0.4	21.3 ± 1.0	22.2

^a The error limits are standard deviations.

Table 7. Summary of Low Rate Dynamic Advancing Contact Angles of Water ($\gamma_{lv} = 72.2$ mJ/m²) on SAlkMI Copolymers and the Corresponding Solid Surface Tension γ_{sv} ^a

copolymer <i>n</i> -alkyl side chain	mean θ_a (deg)	γ_{sv} (mJ/m ²)
methyl	80.1 ± 0.3	35.0 ± 0.2
ethyl	84.5 ± 1.0	32.3 ± 0.6
propyl	85.6 ± 1.0	31.6 ± 0.6
butyl	90.4 ± 0.6	28.6 ± 0.4
pentyl	90.7 ± 0.7	28.4 ± 0.4
hexyl	93.4 ± 1.3	26.8 ± 0.8
octyl	96.8 ± 1.3	24.7 ± 0.8
dodecyl	100.8 ± 0.5	22.2 ± 0.3

^a The error limits are standard deviations.

**Figure 8.** Solid surface tensions of the PAlkMI and the SAlkMI copolymers as a function of the length of the alkyl side chains.

show similarly a slower decrease from that point. Considering the fact that the surface tension of polyethylene is near 30 mJ/m² and that of closely packed CH₃ groups is near 20 mJ/m²,^{25,35} Figure 8 suggests that the actual surface of both types of copolymers with long side chains is dominated by CH₃ groups. In other words, the wettability of the copolymer films is essentially determined by the long side chains, and the difference in the main chain of the two types of copolymers does not manifest itself in the contact angle any more.

Conclusions

The polarity of the main chain of the backbone of the PAlkMI and SAlkMI copolymers manifests itself in their solid surface tension only for the very short alkyl side chains. For these copolymers, the surface tension of the SAlkMI copolymers is significantly lower than that of the PAlkMI copolymers, indicating shielding of the polar group in the backbone chain by the styrene rings. Above

a chain length of $C = 6$ the surface tensions of the two types of copolymers are essentially equal, suggesting complete shielding of the backbone chain by the alkyl side chains. Beyond $C = 6$, the surface tension decreases only slowly and tends toward a value typical for surfaces made up of CH_3 groups. Apparently, at that point, the side chains are long enough to arrange themselves in a more or less closely packed arrangement, exposing their end groups at the surface. Thermodynamically, this is very plausible as a surface made up of CH_3 groups has the lowest free energy of any polymer or other low-energy material that does not contain fluorine.

Acknowledgment. The support of this work by the "Deutsche Forschungsgemeinschaft" within the "Sonderforschungsbereich 287" is gratefully acknowledged.

References and Notes

- (1) Ward, W.; McCarthy, T. J. In *Encyclopedia of Polymer Science and Engineering*, 2nd ed.; Mark, H. F., Bikales, N. M., Overberger, C. G., Menges, G., Kroschwitz, J. I., Eds.; John Wiley and Sons: New York, 1989; Suppl. Vol., p 674.
- (2) Chen, W.; McCarthy, T. J. *Macromolecules* **1997**, *30*, 78.
- (3) Wienhold, U. Ph.D. Thesis, Martin-Luther-Universität Halle-Wittenberg, Halle, Germany 1994.
- (4) Häussler, L.; Wienhold, U.; Albrecht, V.; Zschoche, S. *Thermochim. Acta* **1996**, *277*, 17.
- (5) Kwok, D. Y.; Li, A.; Lam, C. N. C.; Wu, R.; Zschoche, S.; Pöschel, K.; Gietzelt, T.; Grundke, K.; Jacobasch, H.-J.; Neumann, A. W. *Macromol. Chem. Phys.* **1999**, *200*, 1121.
- (6) Hendlinger, P.; Laschewsky, A.; Bertrand, P.; Delcorte, A.; Legras, R.; Nysten, B.; Möbius, D. *Langmuir* **1997**, *13*, 310.
- (7) Bliznyuk, V. N.; Ponomarev, I. I.; Rusanov, A. L. *Thin Solid Films* **1994**, *237*, 231.
- (8) Kakimoto, M.; Imai, Y. *Macromol. Symp.* **1995**, *98*, 1123.
- (9) Fowler, M. T.; Suzuki, M.; Engel, A. K.; Asano, K.; Itoh, T. *J. Appl. Phys.* **1987**, *62*, 3427.
- (10) Dörr, M.; Zentel, R.; Dietrich, R.; Meerholz, K.; Bräuchle, C.; Wichern, J.; Zippel, S.; Boldt, P. *Macromolecules* **1998**, *31*, 1454.
- (11) Kwok, D. Y.; Neumann, A. W. *Adv. Colloid Interface Sci.* **1999**, *81*, 167.
- (12) Spelt, J. K.; Li, D. In *Applied Surface Thermodynamics*; Neumann, A. W., Spelt, J. K., Eds.; Marcel Dekker: New York, 1996; p 239.
- (13) Mach, P.; Huang, C. C.; Stoebe, T.; Wedell, E. D.; Nguyen, T.; de Jeu, W. H.; Guittard, F.; Naciri, J.; Shashidar, R.; Clark, N.; Jiang, I. M.; Kao, F. J.; Liu, H.; Nohira, H. *Langmuir* **1998**, *14*, 4330.
- (14) Hwang, S. S.; Ober, C. K.; Perutz, S.; Iyengar, D.; Schneggenburger, L. A.; Kramer, E. J. *Polymer* **1995**, *36*, 1321.
- (15) Iyengar, D.; Perutz, S. M.; Dai, C.-A.; Ober, C. K.; Kramer, E. J. *Macromolecules* **1996**, *29*, 1229.
- (16) Chapman, T. M.; Benrashid, R.; Marra, K. G.; Keener, J. P. *Macromolecules* **1995**, *28*, 331.
- (17) Chapman, T. M.; Marra, K. G. *Macromolecules* **1995**, *28*, 2081.
- (18) Wang, J.; Mao, G.; Ober, C. K.; Kramer, E. J. *Macromolecules* **1997**, *30*, 1906.
- (19) Pospiech, D.; Jehnichen, D.; Häussler, L.; Voigt, D.; Grundke, K.; Ober, C. K.; Körner, H.; Wang, J. *Polym. Prepr. (Am. Chem. Soc., Div. Polym. Chem.)* **1998**, *39*, 882.
- (20) Chapman, T. M.; Marra, K. G. *Macromolecules* **1995**, *28*, 2081.
- (21) Chapman, T. M.; Benrashid, R.; Marra, K. G.; Keener, J. P. *Macromolecules* **1995**, *28*, 331.
- (22) Marra, K. G.; Chapman, T. M.; Orban, J. M. *Macromolecules* **1996**, *29*, 7553.
- (23) Huang, H.; Marra, K. G.; Ho, T.; Chapman, T. M.; Gardella, J. A., Jr. *Macromolecules* **1996**, *29*, 1660.
- (24) Augsburg, A.; Grundke, K.; Pöschel, K.; Jacobasch, H.-J.; Neumann, A. W. *Acta Polym.* **1998**, *49*, 417.
- (25) Wulf, M.; Grundke, K.; Kwok, D. Y.; Neumann, A. W. *J. Appl. Polym. Sci.* **2000**, *77*, 2493.
- (26) Kwok, D. Y.; Gietzelt, T.; Grundke, K.; Jacobasch, H.-J.; Neumann, A. W. *Langmuir* **1997**, *13*, 2880.
- (27) Del Rio, O. I.; Kwok, D. Y.; Wu, R.; Alvarez, J. M.; Neumann, A. W. *Colloids Surf.* **1998**, *A 143*, 197.
- (28) Kwok, D. Y.; Neumann, A. W. *Prog. Colloid Polym. Sci.* **1998**, *109*, 170.
- (29) Lam, C. N. C.; Ko, R. H. Y.; Yu, L. M. Y.; Li, D.; Hair, M. L.; Neuman, A. W. Dynamic Cycling Contact Angle (DCCA) Measurements: Study of Advancing and Receding Contact Angles. Submitted for publication.
- (30) Lam, C. N. C.; Kim, N.; Hui, D.; Kwok, D. Y.; Hair, M. L.; Neumann, A. W. Liquid Retention on the Solid as a Cause of contact Angle Hysteresis. Submitted for publication.
- (31) Kwok, D. Y.; Lam, C. N. C.; Li, A.; Zhu, K.; Wu, R.; Neumann, A. W. *Polym. Eng. Sci.* **1998**, *38*, 1675.
- (32) Schmidt, M. W.; Baldrige, K. K.; Boatz, J. A.; Jensen, J. H.; Koseki, S.; Gordon, M. S.; Ngyuen, K. A.; Windus, T. L.; Elbert, S. T. *Quantum Chem. Prog. Exch. Bull.* **1990**, *10*, 52.
- (33) Friedel, P. Unpublished work.
- (34) Li, D.; Neumann, A. W. *Applied Surface Thermodynamics*; Neumann, A. W., Spelt, J. K., Eds., Marcel Dekker Inc.: New York, 1996; Chapter 12, p 557.
- (35) Neumann, A. W. *Adv. Colloid Interface Sci.* **1974**, *4*, 105.

MA0021592